THE JOURNAL OF PHYSICAL CHEMISTRY C

Article

pubs.acs.org/JPCC

Tetrahedral Au_{17}^+: A Superatomic Molecule with a Au_{13} FCC Core

Lijuan Yan,[†] Longjiu Cheng,*[,‡] and Jinlong Yang*[,†]

[†]Hefei National Laboratory for Physics Sciences at the Microscale, University of Science & Technology of China, Hefei, Anhui 230026, PR China

[‡]Department of Chemistry, Anhui University, Hefei, Anhui 230601, RP China

Supporting Information

ABSTRACT: A unique tetrahedral structure of Au_{17}^+ (T_d) is found by using first-principles global optimization, which lies 0.40 eV lower in energy than the previously known structure and has a fairly large HOMO−LUMO gap (1.46 eV) at the TPSS/def2-TZVP level. For neutral Au_{17}, this tetrahedral structure is distorted to D_{2d} symmetry but is also 0.18 eV lower in energy than the previous flat cage structure. Au_{17}^+ (T_d) has a FCC Au_{13} octahedral core, and the other four gold atoms are above its four triangular faces. Magic electronic stability of the cluster is explained by the super valence bond model, of which it can be seen as a superatomic molecule in the electronic structure. Moreover, the cluster can also be viewed as a network of eight 2e-superatoms. This Au_{17}^+ cluster mimics the behavior of the Au_{20} pyramid, known as a unique one among the family of gold clusters since its discovery in 2003, in electronic structures.

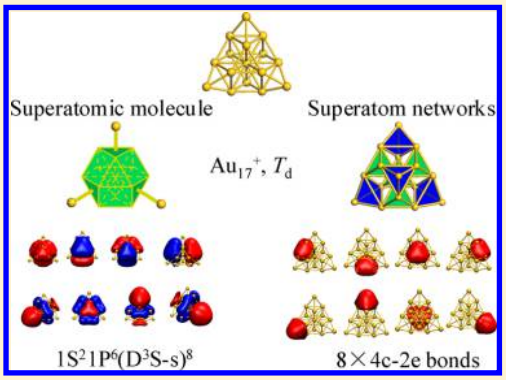

1. INTRODUCTION

Gold clusters and nanoparticles have been a hot issue during the past few years due to their particular properties, such as the unique size-dependent catalytic activity, relativistic effects, aurophilic attraction, and hyperfine properties,[1,2] and many experimental and theoretical investigations surged on this aspect.[3−6] Due to the strong relativistic effects, Au clusters have very unique geometric properties compared to other coinage metals. Small Au clusters display unique planar structures at about n = 2−10,[7,8] a transition from 2D to 3D structures at n = 11−13,[9,10] flat cage at n = 14−19,[11−13] pyramidal cage for Au_{20},[14] golden fullerene for Au_{32},[15,16] and the core−shell structure at n = 33−38.[17] Similar 2D-to-3D structural transitions are also viewed for Au cluster cations and anions, but the transition sizes are different.[5,6]

Electronic shells of metallic clusters can be understood by the Jellium model,[18,19] which assumes a uniform background of positive charge of the cluster's atomic nuclei and the innermost electrons, in which valence electrons move and are subjected to an external potential. Thereby, the whole cluster can be viewed as a "superatom". The appropriate aufbau rule of super shells for spherical Au clusters is $|1S^2|1P^6|1D^{10}|2S^2 1F^{14}|$, etc., associated with magic numbers 2, 8, 18, 34, etc.[20]

Among Au clusters, Au_{20} is very unique in geometry,[14] which possesses a pyramidal structure (T_d) and is a small piece of the face-centered-cubic (fcc) lattice of bulk gold at a small relaxation. It has a remarkably large energy gap (1.77 eV) between the highest occupied and lowest unoccupied molecular orbitals (H−L), suggesting high electronic stability. The full-filled 5d electrons of Au ($5d^{10}6s^1$) are mainly localized as lone-pairs (LPs) and $6s^1$ are free valence electrons, and there are 20 free electrons in Au_{20}, which, however, does not follow the magic number (18e) in the spherical Jellium model.

To understand the magic stability of the Au_{20} pyramid, King et al.[21] thought that the 20 free electrons can be used to form a 4-center 2-electron (4c−2e) bond in each of the 10 tetrahedral cavities of the Au_{20} cluster (four at the vertices and six at the edges). Later, such a conjugated 4c−2e bonding model was confirmed by chemical bonding analysis.[22] Au_{20} can also be viewed as a network of ten 2e-superatoms (10 × 2e) based on the superatom-network (SAN) model.[23] More recently, based on the newly proposed super valence bond (SVB) model,[24−26] Au_{20} is proven to be a superatomic molecule bonded by one 16c−16e Au_{16} superatom and four Au atoms.[27]

Since the discovery in 2003,[14] the Au_{20} pyramid is taken as an exception different from any other Au clusters. However, in this work, we find a sister of it by using density functional theory (DFT) calculations: tetrahedral Au_{17}^+ cluster. It is analogous to Au_{20} in electronic properties and can be viewed as a superatomic molecule based on the SVB model.

2. COMPUTATIONAL METHODS

The structures are located by unbiased global search of the potential energy surface using the genetic algorithm (GA)[28−30] at the DFT level. DFT calculations are carried out on Gaussian 09 package,[31] using the generalized gradient approximation method by Tao−Perdew−Staroverov−Scuseria (TPSS)[32] with relativistic effective core potential basis set (def2-TZVP). The

Received: August 14, 2015
Revised: September 23, 2015
Published: September 24, 2015

DOI: 10.1021/acs.jpcc.5b07917
J. Phys. Chem. C 2015, 119, 23274−23278

calculated H-L gap (1.91 eV) of Au_{20} pyramid at the TPSS/def2-TZVP level is in good agreement with the experimental value (1.77 eV).[14]

3. RESULTS AND DISCUSSION

Tetrahedral Au_{17}^+ (**I**) also has a high T_d symmetry and has an octahedral Au_{13} core. The Au_{13} octahedron is a FCC fragment, which has six square faces and eight triangular faces. The other four gold atoms are above the non-nearest neighbor triangles (Figure 1). The calculated H-L gap of the tetrahedral Au_{17}^+ is

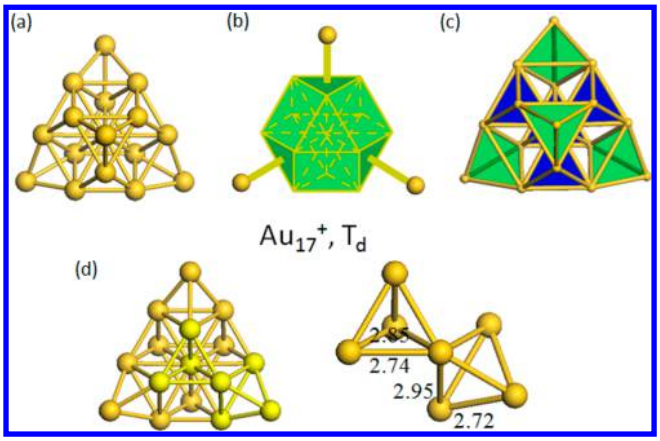

Figure 1. (a) Geometric structure, (b) superatomic molecule model, (c) 8 × 2e SAN model, and (d) the Au−Au bond lengths (Å) in the Au_4 tetrahedron of the tetrahedral Au_{17}^+ (**I**).

also fairly large (1.46 eV), indicating high electronic stability. The other nine low-energy isomers (**II**-**IX**) located in the unbiased global search are plotted in Figure 2a, which are 0.40−0.60 eV higher in energy. Isomer **X** is based on the Au_{20} pyramid, which is not located in the unbiased search due to its high energy (0.91 eV). It should be noted that the structures and their energetic order of gold clusters are very sensitive on the functional, and it was found that the TPSS functional agrees well with the high level coupled cluster method for small charged Au clusters.[33,34] The high level wave function method cannot be performed due to the large size of the current system. However, for each DFT methods with and without dispersion interaction, isomer **I** is the energy lowest one (Table S1).

Experimentally, the information on cluster structures cannot be given directly, but some physical properties are measured by ion-mobility or trapped ion electron diffraction methods, and the structural information is deduced from the comparison of the simulated values from DFT-predicted structures and the experimental values.[5,6,35] Previously, isomer **IV** is found in maximal agreement with the experimental data in simulated and experimental reduced molecular scattering functions.[35] However, isomer **I** is not successfully predicted in previous works and is even 0.54 eV lower in energy than isomer **IV**. To further verify the newly predicted tetrahedral cluster, energies of isomers **I** and **IV** are compared by the wave functional method, and **I** is 0.59 eV lower in energy than **IV** at the MP4/def2-TZVP level of theory.

For comparison, the low-energy isomers for neutral Au_{17} clusters are also located using the GA-DFT method as plotted in Figure 2b. In the neutral state, the tetrahedral cluster is changed to a D_{2d} symmetry (**a**) due to Jahn−Teller distortion. Interestingly, the previously reported global minimum structure for neutral Au_{17} is (**b**) a flat cage structure,[11] which is 0.18 eV

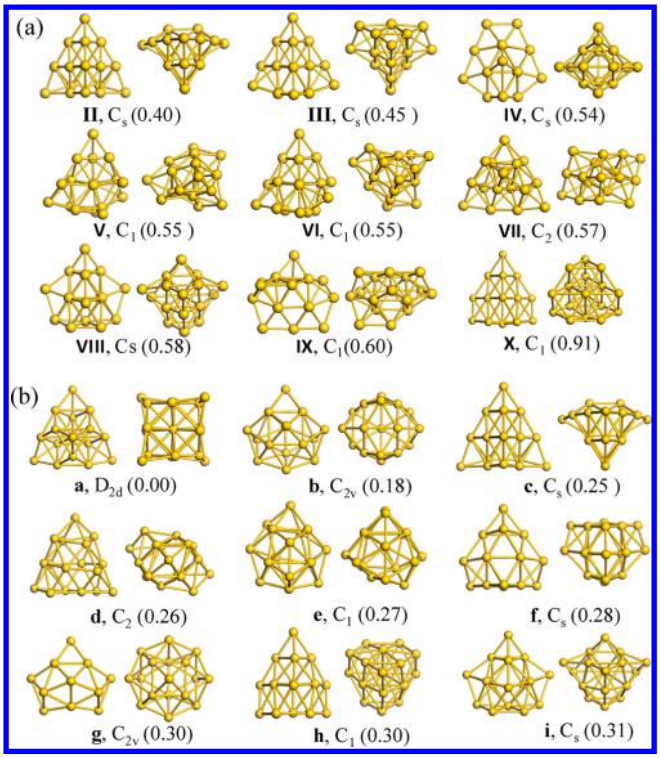

Figure 2. Low-energy isomers of (a) cationic Au_{17}^+ and (b) neutral Au_{17} clusters optimized at the TPSS/def2-TZVP level. Labeled are symmetry and energy (eV) relative to the global minimum one.

higher in energy than the tetrahedral structure at the TPSS/def2-TZVP level [using the same PBE/LANL2DZ method as in ref 11, isomer **a** is also 0.12 eV lower in energy than isomer **b**]. All the isomers are verified to be real local minima by frequency check.

The low energy, large HOMO−LUMO gap, and high symmetry suggest the magic stability of structure **I** to be similar to Au_{20}. Here we first explain the magic electronic stability of **I** by using the SVB model. The octahedral Au_{13}^+ core of **I** is spherical enough and can be viewed as an open-shell 12e-superatom (abbreviated as O). Electronic shells of O ($1S^21P^61D^4$) follow the rule of the spherical Jellium model. Molecule-like electronic shell-closure is achieved by four superatom−atom super bonding (O−Au), and **I** can be viewed as a superatomic molecule OAu_4. Figure 3 gives a schematic representation of the bonding pattern of OAu_4. The $1S^21P^6$

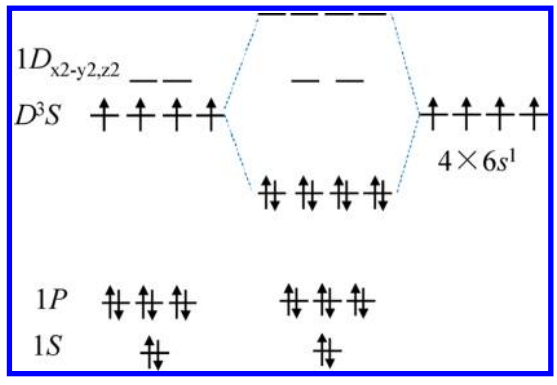

Figure 3. Schematic representation for the D^3S-s bonding superatom−atom in **I**, Au_{17}^+ (OAu_4).

DOI: 10.1021/acs.jpcc.5b07917
J. Phys. Chem. C 2015, 119, 23274−23278

shells of O are super LPs. The five 1D orbitals split into two sets in a tetrahedral field, a set of double-degenerate orbitals ($1D_{x2-y2,z2}$) and a set of triple-degenerate orbitals ($1D_{xy,yz,zx}$). The two $1D_{x2-y2,z2}$ orbitals are empty. The three $1D_{xy,yz,zx}$ orbitals are in D^3S hybridization with the 2S orbital. The four D^3S super orbitals are bonded with four $6s^1$ orbitals of the vertexal Au atoms, splitting into four occupied lower bonding orbitals and four higher antibonding orbitals. Such a bonding pattern is analogous of a simple molecule TiH_4, where Ti $[3s^23p^6(3d4s)^4]$ is in d^3s hybridization bonded with four H atoms.

The comparison of Kohn−Sham molecular orbital (MO) diagrams of OAu_4 and TiH_4 are given in Figure 4. It is clearly

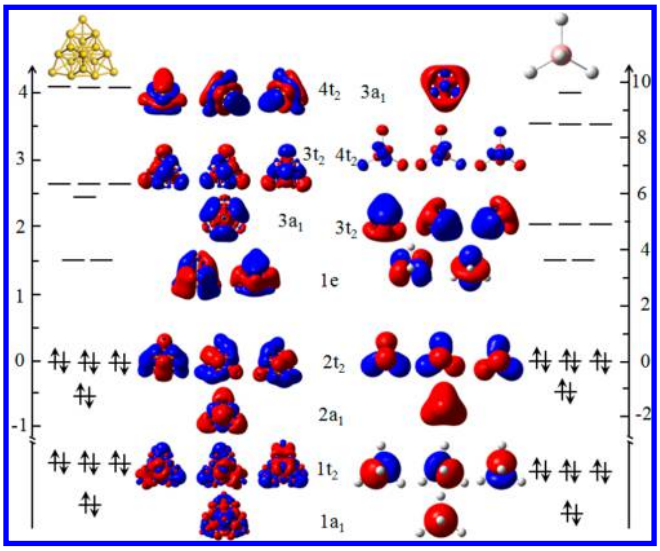

Figure 4. Kohn−Sham MO diagrams of **I**, Au_{17}^+ (left) and TiH_4 (right).

shown that they have similar electronic configurations and orbital shapes. The 1S1P orbitals of superatom O and 3s3p orbitals of atom Ti correspond to $(1a_1)^2(1t_2)^6$ MOs. The unoccupied $1D_{x2-y2,z2}$ orbitals of O and $3d_{x2-y2,z2}$ orbitals of Ti correspond to $(1e)^0$ MOs. The four D^3S-6s, d^3s-1s of O−Au and Os−H bonding orbitals correspond to $(2a_1)^2(2t_2)^6$ MOs, while the four antibonding orbitals are $(3a_1)^0(3t_2)^0$ and $(3t_2)^0(3a_1)^0$ MOs, respectively.

To further confirm the existence of superatom−atom super bonding in **I** (OAu_4), we investigate its chemical bonding patterns using the adaptive natural density partitioning (AdNDP)[36] method. As shown in Figure 5, AdNDP chemical bonding analysis reveals four 13c−2e super LPs in O (super 1S1P) and four 14c-2e super O−Au σ-bonds (D^3S-s), with very high occupancy numbers (ONs > 1.98|e|). As a comparison, a similar bonding pattern of the simple molecule TiH_4, where Ti−H is bonding in d^3s-s hybridization, is also shown.

Under the framework of the SVB model, the superatom−atom bonding in **I** (OAu_4) is very similar to that of Au_{20} (TAu_4), where superatoms O and T are both in D^3S hybridization. The difference is that the super $1D_{x2-y2,z2}$ orbitals are occupied in T but are unoccupied in O. Besides, similar to Au_{20}, electronic structure of the tetrahedral Au_{17}^+ also follows the SAN model. As shown in Figure 6, the 16 free electrons can be used to form a 4c−2e bond in each of the 8 tetrahedral cavities of **I** (4 at vertices and 4 at the body). Thus, the whole cluster can be viewed as a network of eight 2e-superatoms (Au_4

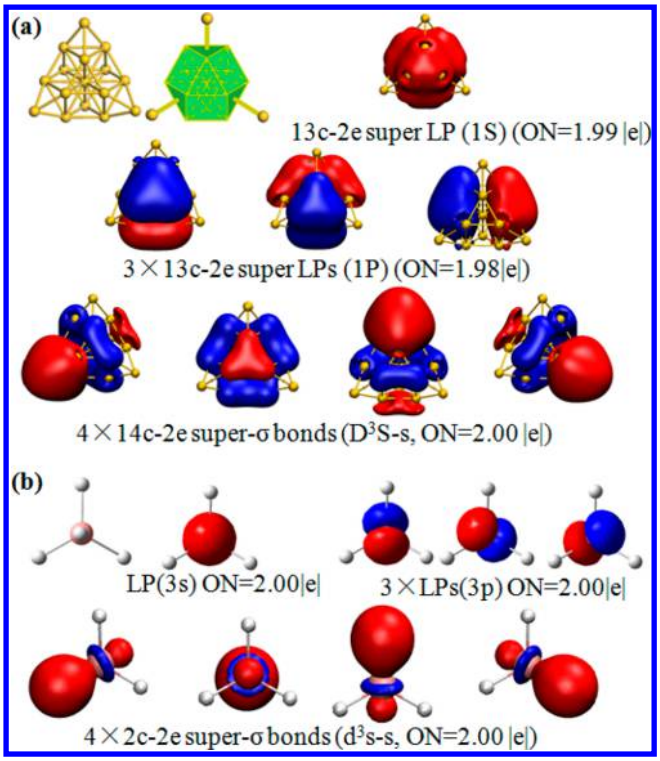

Figure 5. AdNDP chemical bonding of (a) **I**, Au_{17}^+ (OAu4) and (b) TiH_4.

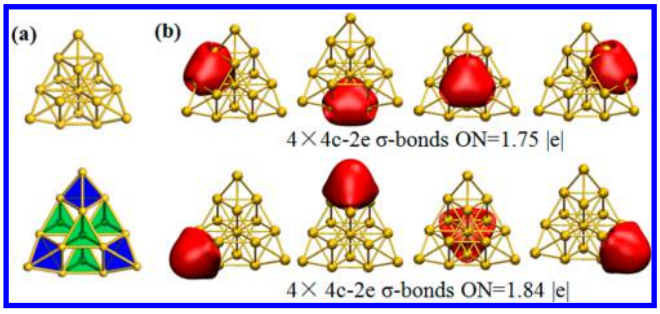

Figure 6. (a) The SAN structure of **I**, Au_{17}^+, and (b) the AdNDP chemical bonding of the 8 × 4c-2e SAN model.

tetrahedron). The vertexal tetrahedron is composed of one vertexal Au atom and three Au atoms in one triangular face of the Au_{13} core. The inner tetrahedron is composed by one central Au atom and three Au atoms in one triangular face. The four inner tetrahedrons share one central Au atom. Each vertexal tetrahedron shares three Au atoms with three inner tetrahedrons.

On the basis of the above geometric analysis, there are two kinds of conjugated 4c-2e Au_4 superatoms (vertexal and inner) existing in Au_{17}^+. AdNDP analysis conforms to such a 8 × 2e SAN model, which reveals eight delocalized 4c-2e σ bonds as shown in Figure 6. ONs of the 4c-2e bonds in vertices are 1.84|e|, while ONs of the inner 4c-2e bonds are 1.75|e|.

To further verify the 8 × 2e SAN model, the nucleus-independent chemical shifts (NICS)[37] values at the center of the Au_4 tetrahedron are calculated. NICS value is a popular measurement of aromaticity, where large negative value denotes aromaticity. NICS values of the vertexal and inner tetrahedrons are −12.73 and −16.63 ppm, respectively, showing high aromaticity. There is also another kind of Au_4 tetrahedrons in

DOI: 10.1021/acs.jpcc.5b07917
J. Phys. Chem. C 2015, 119, 23274−23278

I, which is composed by a triangular face of the vertexal Au_4 tetrahedron and the central Au atom. However, its aromaticity is obviously lower according to NICS values (−7.70 ppm).

On the one hand, the higher aromaticity in the eight Au_4 superatoms indicates certain localization of the electronic density (SAN model). On the other hand, the aromaticity of the nonsuperatom Au_4 tetrahedrons is also fairly high, indicating certain delocalization of the electronic density in the whole Au_{13} octahedron (SVB model). Both SVB and SAN models can give reasonable understanding of the electronic stability of the Au_{20} and Au_{17}^+ clusters. The relationship between SVB and SAN models can be understood by the electronic structure of benzene. The SVB model corresponds to the model of 6c-6e delocalized π bonding, while the SAN model corresponds to the model of three conjugated 2c-2e π bonds. The two models are not in conflict with each other. The SVB model focuses on the delocalized multicentered bonding throughout the whole cluster, while the SAN models tend to the delocalized multicentered bonding between a part of the cluster, which can be viewed as a superatom. Then, the spherical symmetry or nearly spherical symmetry geometric structure of a cluster is needed in the SVB model, but this is usually not necessary in the SAN model. Sometimes, a cluster can be explained well in the SAN model yet not in the SVB model due to the whole geometric structure. In the SVB model, the ONs are close to the idealized value (2.0|e|), indicating high reliability. However, the fairly large ONs in the SAN model (1.75−1.84|e|) indicate certain localization of the 16 valence electrons. Thus, we think that, both models are reasonable, but the superatomic model gives more useful insight from the view of chemical bonding.

4. CONCLUSIONS

In summary, we find a unique structure of gold cluster cation Au_{17}^+ based on DFT calculations. This cluster is in T_d symmetry composed by an octahedral FCC Au_{13} core and four vertexal Au atoms. On the basis of the SVB model, Au_{17}^+ can be viewed as a superatomic molecule (OAu_4) bonded by one 13c−12e superatom and four vertexal Au atoms, and it is an exact analogue of the TiH_4 molecule. On the basis of the SAN model, eight 4c-2e superatoms are divided into two groups, alternately linking to each other, forming a network of tetrahedral 2e-superatoms. The tetrahedral Au_{17}^+ clusters is the only known sister of the famous Au_{20} pyramid, where the two clusters are similar in electronic structures.

■ ASSOCIATED CONTENT

Supporting Information

The Supporting Information is available free of charge on the ACS Publications website at DOI: 10.1021/acs.jpcc.5b07917.

The calculated TD-DFT optical absorption spectra of tetrahedral Au_{17}^+ and Au_{20} clusters, comparison of various functionals in relative energies, and the *xyz* coordinates of the low-energy isomers of Au_{17}^+ and Au_{17} clusters (PDF)

■ AUTHOR INFORMATION

Corresponding Authors

*E-mail: clj@ustc.edu.

*E-mail: jlyang@ustc.edu.cn

Author Contributions

The manuscript was written through contributions of all authors. All authors have given approval to the final version of the manuscript.

Notes

The authors declare no competing financial interest.

■ ACKNOWLEDGMENTS

This work is partially supported by the National Key Basic Research Program (2011CB921404), by NSFC (21273008, 25621421063, 91021004, 21233007, 21573001), by Chinese Academy of Sciences (CAS) (XDB01020300), and by AHUSCC, USTCSCC, SCCAS, Tianjin, and Shanghai Supercomputer Centers.

■ REFERENCES

(1) Pyykkö, P. Theoretical Chemistry of Gold. III. *Chem. Soc. Rev.* **2008**, *37*, 1967−1997.

(2) Shaw, C. F. Gold-Based Therapeutic Agents. *Chem. Rev.* **1999**, *99*, 2589−2600.

(3) Lechtken, A.; Neiss, C.; Kappes, M.; Schooss, D. Structure Determination of Gold Clusters by Trapped Ion Electron Diffraction: Au_{14}^-−Au_{19}^-. *Phys. Chem. Chem. Phys.* **2009**, *11*, 4344−4350.

(4) Assadollahzadeh, B.; Schwerdtfeger, P. A Systematic Search for Minimum Structures of Small Gold Clusters Au_n (n = 2−20) and Their Electronic Properties. *J. Chem. Phys.* **2009**, *131*, 064306.

(5) Furche, F.; Ahlrichs, R.; Weis, P.; Jacob, C.; Gilb, S.; Bierweiler, T.; Kappes, M. The Structures of Small Gold Cluster Anions as Determined by a Combination of Ion Mobility Measurements and Density Functional Calculations. *J. Chem. Phys.* **2002**, *117*, 6982−6990.

(6) Gilb, S.; Weis, P.; Furche, F.; Ahlrichs, R.; Kappes, M. Structures of Ssmall Gold Cluster Cations (Au_n^+, n < 14): Ion Mobility Measurements Versus Density Functional Calculations. *J. Chem. Phys.* **2002**, *116*, 4094−4101.

(7) De, H.; Krishnamurty, S.; Mishra, D.; Pal, S. Finite Temperature Behavior of Gas Phase Neutral Au_n (3 < n < 10) Clusters: A First Principles Investigation. *J. Phys. Chem. C* **2011**, *115*, 17278−17285.

(8) Olson, R.; Varganov, S.; Gordon, M.; Metiu, H.; Chretien, S.; Piecuch, P.; Kowalski, K.; Kucharski, S.; Musial, M. Where Does the Planar-to-Nonplanar Turnover Occur in Small Gold Clusters? *J. Am. Chem. Soc.* **2005**, *127*, 1049−1052.

(9) Spivey, K.; Williams, J.; Wang, L. Structures of Undecagold Clusters: Ligand Effect. *Chem. Phys. Lett.* **2006**, *432*, 163−166.

(10) Gruber, M.; Heimel, G.; Romaner, L.; Bredas, J.; Zojer, E. First-Principles Study of the Geometric and Electronic Structure of Au_{13} Clusters: Importance of the Prism Motif. *Phys. Rev. B: Condens. Matter Mater. Phys.* **2008**, *77*, 165411.

(11) Bulusu, S.; Zeng, X. Structures and Relative Stability of Neutral Gold Clusters: Au_n (n = 15−19). *J. Chem. Phys.* **2006**, *125*, 154303.

(12) Gruene, P.; Rayner, D. M.; Redlich, B.; van der Meer, A. F.; Lyon, J. T.; Meijer, G.; Fielicke, A. Structures of Neutral Au_7, Au_{19}, and Au_{20} Clusters in the Gas phase. *Science* **2008**, *321*, 674−676.

(13) Gao, Y.; Shao, N.; Pei, Y.; Chen, Z.; Zeng, X. Catalytic Activities of Subnanometer Gold Clusters (Au_{16}-Au_{18}, Au_{20}, and Au_{27}-Au_{35}) for CO Oxidation. *ACS Nano* **2011**, *5*, 7818−7829.

(14) Li, J.; Li, X.; Zhai, H.; Wang, L. Au_{20}: A Tetrahedral Cluster. *Science* **2003**, *299*, 864−867.

(15) Johansson, M.; Sundholm, D.; Vaara, J. Au_{32}: A 24-Carat Golden Fullerene. *Angew. Chem., Int. Ed.* **2004**, *43*, 2678−2681.

(16) Gu, X.; Ji, M.; Wei, S. H.; Gong, X. Au_N Clusters (N = 32,33,34,35): Cagelike Structures of Pure Metal Atoms. *Phys. Rev. B: Condens. Matter Mater. Phys.* **2004**, *70*, 205401.

(17) Shao, N.; Huang, W.; Gao, Y.; Wang, L.; Li, X.; Wang, L.; Zeng, X. Probing the Structural Evolution of Medium-Sized Gold Clusters: Au_n^-(n = 27−35). *J. Am. Chem. Soc.* **2010**, *132*, 6596−6605.

DOI: 10.1021/acs.jpcc.5b07917
J. Phys. Chem. C 2015, 119, 23274−23278

(18) Knight, W.; Clemenger, K.; de Heer, W. A.; Saunders, W. A.; Chou, M.; Cohen, M. Electronic Shell Structure and Abundances of Sodium Clusters. *Phys. Rev. Lett.* **1984**, *52*, 2141−2143.
(19) de Heer, W. A. The Physics of Simple Metal Clusters: Experimental Aspects and Simple Models. *Rev. Mod. Phys.* **1993**, *65*, 611.
(20) Walter, M.; Akola, J.; Lopez-Acevedo, O.; Jadzinsky, P. D.; Calero, G.; Ackerson, C. J.; Whetten, R. L.; Gronbeck, H.; Hakkinen, H. A Unified View of Ligand-Protected Gold Clusters as Superatom Complexes. *Proc. Natl. Acad. Sci. U. S. A.* **2008**, *105*, 9157−9162.
(21) King, R. B.; Chen, Z.; Schleyer, P. Structure and Bonding in the Omnicapped Truncated Tetrahedral Au_{20} Cluster: Analogies between Gold and Carbon Cluster Chemistry. *Inorg. Chem.* **2004**, *43*, 4564−4566.
(22) Zubarev, D. Y.; Boldyrev, A. I. Deciphering Chemical Bonding in Golden Cages. *J. Phys. Chem. A* **2009**, *113*, 866−868.
(23) Cheng, L.; Yuan, Y.; Zhang, X.; Yang, J. Superatom Networks in Thiolate-Protected Gold Nanoparticles. *Angew. Chem., Int. Ed.* **2013**, *52*, 9035−9039.
(24) Cheng, L.; Yang, J. New Insight into Electronic Shells of Metal Clusters: Analogues of Simple Molecules. *J. Chem. Phys.* **2013**, *138*, 141101.
(25) Cheng, L.; Ren, C.; Zhang, X.; Yang, J. New Insight into Electronic Shell of $Au_{38}(SR)_{24}$: a Superatomic Molecule. *Nanoscale* **2013**, *5*, 1475−1478.
(26) Yuan, Y.; Cheng, L.; Yang, J. Electronic Stability of Phosphine-Protected Au_{20} Nanocluster: Superatomic Bonding. *J. Phys. Chem. C* **2013**, *117*, 13276−13282.
(27) Cheng, L.; Zhang, X.; Jin, B.; Yang, J. Superatom−Atom Super-Bonding in Metallic Clusters: A New Look to the Mystery of an Au_{20} Pyramid. *Nanoscale* **2014**, *6*, 12440−12444.
(28) Hartke, B. Global Geometry Optimization of Clusters Using Genetic Algorithms. *J. Phys. Chem.* **1993**, *97*, 9973−9976.
(29) Deaven, D. M.; Ho, K. M. Molecular-Geometry Optimization with a Genetic Algorithm. *Phys. Rev. Lett.* **1995**, *75*, 288−291.
(30) Roberts, C.; Johnston, R. L. Investigation of the Structures of MgO Clusters Using a Genetic Algorithm. *Phys. Chem. Chem. Phys.* **2001**, *3*, 5024−5034.
(31) Frisch, M. J.; Trucks, G. W.; Schlegel, H. B.; Scuseria, G. E.; Robb, M. A.; Cheeseman, J. R.; Scalmani, G.; Barone, V.; Mennucci, B.; Petersson, G. A. et al. *Gaussian 09*, revision B.01; Gaussian, Inc.: Wallingford, CT, 2009.
(32) Tao, J.; Perdew, J. P.; Staroverov, V. N.; Scuseria, G. E. Climbing the Density Functional Ladder: Nonempirical Meta−Generalized Gradient Approximation Designed for Molecules and Solids. *Phys. Rev. Lett.* **2003**, *91*, 146401.
(33) Johansson, M.; Lechtken, A.; Schooss, D.; Kappes, M.; Furche, F. 2D-3D Transition of Gold Cluster Anions Resolved. *Phys. Rev. A: At., Mol., Opt. Phys.* **2008**, *77*, 053202.
(34) Mantina, M.; Valero, R.; Truhlar, D. G. Validation Study of the Ability of Density Functionals to Predict the Planar-to-Three-Dimensional Structural Transition in Anionic Gold Clusters. *J. Chem. Phys.* **2009**, *131*, 64706.
(35) Schooss, D.; Weis, P.; Hampe, O.; Kappes, M. Determining the Size-Dependent Structure of Ligand-Free Gold-cluster ions. *Philos. Trans. R. Soc., A* **2010**, *368*, 1211−1243.
(36) Zubarev, D.; Boldyrev, A. Developing Paradigms of Chemical Bonding: Adaptive Natural Density Partitioning. *Phys. Chem. Chem. Phys.* **2008**, *10*, 5207−5217.
(37) Schleyer, P.; Maerker, C.; Dransfeld, A.; Jiao, H.; Hommes, N. Nucleus-Independent Chemical Shifts: a Simple and Efficient Aromaticity Probe. *J. Am. Chem. Soc.* **1996**, *118*, 6317−6318.

DOI: 10.1021/acs.jpcc.5b07917
J. Phys. Chem. C 2015, 119, 23274−23278